RSC Advances

ROYAL SOCIETY
OF CHEMISTRY

www.rsc.org/advances

Study of different-sized sulfur-free expandable graphite on morphology and properties of water-blown semi-rigid polyurethane foams

Wei Luo, Yi Li, HuaweiZou[*], Mei Liang [*]

The State Key Laboratory of Polymer Materials Engineering, Polymer Research Institute of Sichuan University, Chengdu 610065, People's Republic of China

Abstract： In this paper, EG with different nominal particle sizes (70μm, 430μm and 960μm) and different loading from 0 to 50pphp were considered to investigate the effect of expandable graphite on the morphology and properties of water-blown semi-rigid polyurethane foams (SPFs). Experimental results showed that higher content of EG in the SPF was more conducive to the formation of barrier layer after expansion and exhibited better flame retardancy. Horizontal burning test confirmed the conclusion that the EG-430μm and EG-960μm with various loading could effectively enhance the flame retardant properties of the SPFs. However, EG-70μm could not improve the fire behavior of the composite due to a weak ability to form efficient char layer on the surface of the SPF. Thermo gravimetric analysis (TGA) indicated that EG had a positive effect on the thermal stability of SPFs. In addition to the flame retardant behavior, effects of EG on the density, pore structure, thermal properties, mechanical properties and damping properties of the SPFs were also investigated.

Key words: Expandable graphite, semi-rigid polyurethane foam, flame retardancy, mechanical properties

1 INTRODUCTION

Serving as one of the most important commercial products of polyurethanes,

semi-rigid polyurethane foams(SPFs) is a material with very interesting properties such as low density, high specific strength and good energy absorption capacity, and now have been widely used as interior materials of automobile, industrial cushioning material and packaging materials. [1-4] However, SPFs is a highly flammable material due to the porous, open-cell structure, low degree of crosslinking and low density, which limits its further use in many fields. [5] Incorporation of flame-retardant additives into foams is the most popular approach to improve flame retardancy of polyurethane foams (PUFs). Recently, large range of flame retardants such as halogen, phosphorus, and nitrogen based compounds are used in PUFs [6]. Due to the highly toxic and potentially carcinogenic brominated furans and dioxins formed during combustion, halogen based compounds，as a high efficiency fire retardant additive，is currently restricted in SPFs. A great deal of attention has been paid to halogen-free fire retardant additives [7].

Expandable graphite (EG), as a halogen-free flame retardant, is prepared by the intercalation of a variety of intercalation agents [8, 9] and can be rapidly exfoliated, to some extent, hundreds of times over its initial volume when subjected to high temperature, and forming a low density, 'worm-like' morphology **(Figure 2c)**. The 'worm-like' structure forms a low-density, thermal insulating layer on the heating surface which prevents the polymer from further degrading. Because of outstanding effect, EG has been widely used as flame retardant additives in polymers [10-12]. Numbers of studies were reported about EG modified polyurethane foams (PUFs) [13-20]. Unfortunately, these studies are mainly focused on the rigid polyurethane

foam, whereas the effect of EG on modified semi-rigid or flexible polyurethane foams has been few reported. Moreover, great majority of EG are made from sulfuric acid and will release large amounts of SO_2 and SO_3 during its exfoliation process and has corrosive sulfur residual, which limited its applications in nuclear power plants, electronics, aerospace and automobile industries.[21]

Flame retardant properties of the EG/PUF composites depend strongly on the EG size, foam density and the EG content. [22-24] In this paper, three large-span particle sizes of sulfur-free EG (70μm, 430μm, 960μm) were filled into water-blown SPFs with different content as a flame retardant additives. The flame retardant properties and thermal stability of the composites were evaluated by LOI, Underwriters Laboratories 94 (UL-94) [34] standard and thermogravimetric analysis. Dynamic mechanical analysis (DMA) was employed to examine the damping properties of the composites. Moreover, the effects of EG flakes on the viscosity of the reaction mixture, density, morphology and mechanical properties of the foam were also discussed.

2 EXPERIMENTAL

2.1 Raw Materials

Polymethylene polyphenyl isocyanate (PAPI) was supplied by Badische Anilin-und-Soda-Fabrik (BASF) Co. The –NCO content by weight and average functionality are 30.5 and 2.7 respectively. Polyether polyol 3050A was purchased from GaoQiao Petro. Co. (Shanghai, China). According to the manufacturer, typical hydroxyl number is 55.8 mg KOH/g with a functionality of 3. Low molecular weight

polyethylene glycol, used as a chain extender, was synthesized in our laboratory with a functionality of 2. Dabaco DC5188 was used as a surfactant. Catalysts Dabaco 2040 and stannous octoate, employed for the formation of urethane and cyclotrimerization of isocyanate, were purchased from Air Product (China) and Chengdu Chemical Reagent Co. (Chengdu, China). Distilled water was used as a chemical blowing agent. Sulfur-free expandable graphite, with a broad particle size distribution, was provided directly by the manufacturer with a density of $2.2g/cm^3$, ash of 0.9%, moisture of 0.6%, volatile of 10%, pH value of 7.0 and initial expansion temperature at about 160^oC, the digital micrographs of three kinds of EG are shown in **Figure 1**..

Materials used in this work classed into two components as component A and component B. Component A is from a mixture of substances containing polyether polyol, chain extender, surfactants, catalyst, blowing agents, and EG. Component B is isocyanate (PAPI).

2.2 Foam Preparation

Before the foam preparation process, EG was sieved into three different particle sizes by a series of grading sieves. The average nominal particle sizes in diameter of EG used in this study were 70μm, 430μm and 960 μm, which were statistic values based on the micrograph measurement, respectively. The expanded volumes of EG-70μm, EG-430μm, EG-960μm at high temperature are showed in **Figure 2**.

The EG-filled SPFs were prepared through a one-shot, free-rise method. The chemical compositions used to prepare the EG/SPF composite in this study are

presented in **Table 1**. All components except EG and PAPI were mixed and stirred together with an electric stirrer until a uniform mixture was obtained. Then measured EG was added and the mixture (component A) was stirred for 3min. PAPI was added into the mixture in a certain weight ratio and then stirred fast for 15 s. And then the mixture was quickly poured into an cube mold with a dimension of 250mm × 250mm × 250mm. Finally, the foams were aged at room temperature for 24h before characterizations. In this work, The EG loading was from 0 to 50pphp. Foam samples were cut into required shape for the evaluation of different properties.

3 CHARACTERIZATION

3.1 Viscosity of the reaction mixture (component A)

The EG filled component A was analyzed in a dynamic rheometer (Bohlin Gemini 2000, Malvern, British) in the solution state. The samples were studied under a steady-state mode. All of the samples were tested in a frequency sweep range from 0.05 to 100 Hz with a strain of 1%. The samples were added in a parallel-plate with a diameter of 40 mm, and the rheological tests were performed at 25 °C with a gap distance of 1 mm.

3.2 Apparent density

The apparent densities of the samples were carried out according to the standard ISO 845:2006. The values of the apparent density were calculated as a mass/volume ratio.

3.3 Compression test

The compression strength and modulus of all samples were measured with a universal electronic tensile machine (Instron 5507, USA). The size of the specimen was 30 mm×30 mm×30 mm and the rate of compression process was set at 3 mm/min for each sample. The compressive stress at 25% strain in parallel to the foam-rise direction was performed according to the standard ISO 844:2004.

3.4 Morphology characterization

The morphology of the foams before burning was examined through a scanning electron microscope (SEM, JSM-9600, JEOL, Japan) with accelerating voltage of 5kV. Samples were cut into flakes with a blade and then sputter-coated with gold for SEM observations.

The morphology of EG with different sizes and interfaces of burned 50pphp EG/SPF composites were observed by a digital microscope with enhanced depth of field (VHX-1000, KEYENCE, Japan).

3.5 Burning behaviors

The burning behaviors of EG filled SPFs were evaluated by limiting oxygen index test, horizontal and vertical burning test.

The limiting oxygen index (LOI) was measured by a HC-2 oxygen index test instrument (Jiangning, China) according to the standard ISO 4589-2:1996 with a sheet size of 125 mm×10 mm×10mm.

The horizontal and vertical burning test was conducted according to UL-94 and ASTM-D 635 with a sheet size of 125 mm×13 mm×10mm.

3.6 Thermo gravimetric analysis (TGA)

Thermogravimetric measurements were conducted with a thermogravimetric analyzer (NETZSCH TG 209F1 Iris, Germany) under dry nitrogen gas with a flow rate of 60mL/min. The relative mass loss of the samples was recorded from $50^{o}C$ to $650^{o}C$ with a heating rate of $10^{o}C/min$.   The samples had an approximate weight of 4mg.
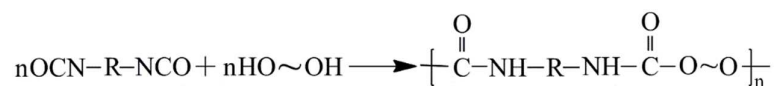
3.7 Dynamic Mechanical Analysis (DMA)

Dynamic mechanical analysis was carried out in a DMA Q800 (TA Instruments, USA). Samples with dimensions of $50mm \times 11mm \times 6$ mm were tested using a cantilever bending model at a frequency of 5 Hz and a heating rate of $3^{o}C/min$ from -95 ^{o}C to $60^{o}C$.

4 RESULTS AND DISCUSSION

4.1 Viscosity of the reaction mixture (Component A)

It is known that the synthetic of the polyurethane follow the equation:

$$nOCN-R-NCO + nHO\sim OH \longrightarrow \left[\overset{O}{\underset{\|}{C}}-NH-R-NH-\overset{O}{\underset{\|}{C}}-O\sim O\right]_n$$

In the processing and preparation of SPF by the one-shot, free-rise method, component B was added into component A and then high speed stirring about 2000rpm was used to promote this synthesis reaction (see 2.2). In this case, the viscosity of component A

plays a crucial role in the molding process **[22]**. Excessive high viscosity of component

A will cause incomplete reaction during the foaming and slow the rise of the foam. To

study the effect of EG on the viscosity of the component A and eliminate its effects on

the molding process of SPF, we conducted viscosity tests on the component A before

the foam preparation. As shown in **Figure 3**, it is clear that EG-70μm had a greater

tackify effect on the viscosity of component A than EG-430μm and EG-960μm. Such

phenomenon could be attributed to the larger numbers of EG-70μm particles, which

obstructed the movement of molecular chains. As the EG content increased from 0 to

50pphp, the viscosity of EG-70μm filled component A showed a dramatic increase

from 1.58 Pa·s to 45.05 Pa.s, while this values were only 5.48 Pa·s and 3.49 Pa·s for

the other two samples. Moreover, viscosity of the component A decreased gradually

with the increase of shear rate, this was anticipated due to the orientation of the

molecular chains and graphite flakes during the test.

4.2 Density and mechanical properties

Foam density is a very important parameter, which affects the mechanical

properties of polyurethane foams. **[25]** What had been demonstrated is that strength,

modulus and energy absorption abilities of a material improve linearly with the increase

of foam density. **[23]** Consequently, the density of polyurethane foam materials, to a

great degree, determines SPF's applications. As shown in **Figure 4**, increasing the

amount of EG in SPF from 5pphp to 50pphp resulted in a distinct increase in the

apparent density of the foam, because the higher density of EG ($2.2g/cm^3$) than that of

the neat SPF. However, three particle size of EG showed a different effect on the density of SPF. The density of the SPF filled with EG-70μm increased from 76.42 kg/m^3 for the neat foam to 116.18 kg/m^3, which was greater than that of EG-430μm/SPF and EG-960μm/SPF composites. This was probably due to the fact that the smaller particle size of EG had a "nucleating" effect during the foam formation, and then the average cell size of the composite decreased. Similar result was reported in Bian Xiang-Cheng's study. **[23]**

As a materials used in packaging industry, mechanical properties are particular important parameters in determination of the SPF's applications. However, it has been reported incorporating filler into polyurethane foam results in inferior mechanical properties, and the distribution of filler in the matrix largely determines the performance of the composites. **[26]** In the present case, the effect of EG flake loading on the compressive strength properties of SPF was studied by the specific compressive strength (compressive strength/density) measurement. **Table 2** and **Figure 4** show the specific compressive strength and compressive strength at 25% strain of the EG/SPF composite with different EG loadings. It is clear that SPFs filled with EG-70μm demonstrated an erratic increase in compressive strength while the other two systems showed a slight decrease. The increase in compressive strength of EG-70μm/SPF composite could be mainly due to the increase in the density. The presence of EG-70μm in the foam matrix restricted the deformation of the foam. However, the loading of EG-430μm and EG-960μm distributed between the cell walls and formed many defects in composite, which attribute to the weak adhesion between the graphite flakes and the

foam matrix **(Figure 5(d))**. As a result, the compressive strength of EG-70μm/SPF composites increased while the other two systems showed a slight decrease.

It was noted that the trend of apparent density and compression strength of EG/SPF composite were similar as the increase in EG loading. It suggested that changes in the mechanical strength of the foam were greatly related to the corresponding foam density.

4.3 Morphology analysis

In general, the mechanical properties of foam depend on not only the rigidity of the polymer matrix but also the cell morphology of foam. Therefore, it is of interest to observe the morphology of foam. **Figure 5a** show the SEM cell micrograph of pure SPF. The open-cell structure could be found clearly in the neat SPF. Besides, and no collapse was observed in the cell system, indicating that the pure foam had a uniform cell structure.

As presented in **Figure 5b**, the small graphite flakes were intercalated and dispersed uniformly in the foam matrix. It is seen that the cells were not as regular as those in neat SPF, but are approximately spherical. As shown in **Figure 5(c~ d)**, when the particle size of EG was in the same order as the cell, all the graphite flakes did not located in the struts but between the cell walls even at 50pphp loading amount. This result was in good agreement with the study of EG-containing rigid polyurethane foam. **[16, 22]** For different particle size and loading of EG, no obvious cell bubble collapse was observed in the composites.

To better understand the distribution of the graphite in the foam, a digital microscope with enhanced depth of field was employed to observe the foam surface. As shown in **Figure 6(a ~ c)**, the increase in particle size of EG led to a decrease of graphite particle numbers in the foam (50pphp).This decrease also indicated the uniformly distribution of EG particles. Furthermore, it could be deduced that the stirring process during the foam preparation had a damaging effect on the graphite flakes according to the micrographs **(Figure 6c)**.

Obvious gaps existed between the graphite flakes and SPF matrix as the arrow shown in **Figure 6d**, indicating the poor interaction between the EG particles and the organic foam matrix.

4.4 Combustion properties

Limiting oxygen index (LOI), horizontal and vertical burning tests were employed to investigate the flame retardant behavior of EG/SPF composites.

4.4.1 Limiting Oxygen Index measurement

The LOI curves of EG filled SPFs are shown in **Figure 7**. As the EG loading increased from 0 to 50 pphp, the LOI value of the EG-960μm/SPF composites dramatically increased to 31% from 20% while the other two composites were only reached 26% and 21%. This result confirmed our expectancy that higher content and larger particle size of EG was beneficial to the flame retardant properties of SPFs. It was also in good agreement with the previous studies. **[13, 21, 22]**

The flame retardant mechanism of EG/SPF composite is shown in **Figure 8**.

When the composite was subjected to fire, the external graphite expanded fast into a low density, 'worm-like' morphology, and the volume increased more than 200 times instantly. This structure, as shown in **Figure 1**, embedded in the surface and formed thermal insulating layers on the heating surface of the foam. This expanded EG (also called burned layer or char layer) could hinder the oxygen diffusion, limit the heat penetration, and restrict mass transfer from SPF matrix to the heat source, thus prevent the matrix from further degrading. Similar results was reported by Modesti et al. **[14]**

It should be emphasized that the presence of EG-70μm lead the LOI value of the composite first decreased and then increased slowly. This may be attribute to the smaller expansion volume of EG-70μm (**Figure 1**) couldn't form thermal insulating layers and improve the flame retardancy of SPF. What's more, this low-density ineffective barrier layer (**Figure 9**) is beneficial to the air exchange during the combustion and the degradation of SPF matrix promoted. The slight increase of LOI value at high EG loading was related to the increase in apparent density of the foam (see **Figure 3**).

4.4.2 Horizontal and vertical burning test

The results of the horizontal burning tests are tabulated in **Table 3**. According to the test, the procedures include applying the test flame for 30 ± 1 s without changing its position. For the horizontal fire test, the samples can be assigned an "HB" rating if the rate of burning is less than 75 mm/min and the flame is restricted to a length of

100 mm. More specifically, if the flame front did not pass the 25 mm reference mark

and quenches after the ignition source being removed, the rating of the materials

classifications is defined as HB-1. If the flame front passed the 25 mm reference mark

and ceased before 100mm mark, the rating of the materials classifications is defined

as HB-2 and the damaged length should be recorded. If flame front passed the 100

mm mark, the burning rate can be calculated according to the formula below:

$$V = \frac{60L}{t} \tag{1}$$

where **V** represents burning rate (mm/min), **L** denotes burned length (mm) and **t**

means burning time (s) and if the burning rate was less than 40mm/min, the rating of

the materials classifications can be defined as HB-3.

It can be seen that the burning rate of the composites showed a different

response with the content of EG increased from 0 to 50pphp. The EG-70μm showed

almost no effect or even increased on the burning rate of SPF while the EG-430μm

and EG-960μm had a significantly decrease. According to the data in **Table 3**, the

EG-430μm/SPF composite reached the horizontal burning test of HB-3 rating at a

15pphp loading while the EG-960μm/SPF achieved only at the loading of 5pphp.

What's more, only the EG-960μm/SPF composite with 50pphp EG loading could pass

the vertical burning test and classified as V-0 rating because of its good fire retardant

property.

The results of horizontal burning test were in good agreement with the LOI

testing (**Figure 7**). The data also proved that EG with larger particle size and at

higher loading could efficiently improve the flame retardant properties of SPFs for

practical use. The presence of EG-70μm had no improvement, or even negative effect on the flame retardant of SPFs.

4.5 Thermal stability

Figure 10 shows the thermogravimetric (TG) and derivative curves (DTG) behaviors of pure SPF and SPFs filled with three different particle sizes of EG under nitrogen. Both the neat and EG-containing samples took a two-step degradation process from nearly $230^{\circ}C$ to $400^{\circ}C$ [17, 27]. The representative thermal analysis data of the samples are listed in **Table 4**. The initial decomposition temperature ($T_{5wt\%}$) was the temperature at 5% weight loss, while the maximum weight loss temperature (T_{max}) was taken from the peak value of the DTG curve. Results revealed that the presence of EG had a significant increase in $T_{5wt\%}$ of SPF systems. Moreover, the larger size and higher content was conducive to the raise of $T_{5wt\%}$ of the EG-containing SPFs. It is believed the exfoliated graphite flakes formed during the heat treatment process was not beneficial to the penetration of heat, improving the thermal stability of SPFs. Larger particle size of EG and high content in the SPFs have a positive effect on the conformation of the isolation layer which showed higher thermal stability. The DTG thermograms show that SPFs had a slight effect on the value of T_{max} while in the presence of EG. In addition, in the case of SPF/EG, a shoulder peak was observed between $260^{\circ}C$ and $320^{\circ}C$. This may be due to the oxidation and degradation of the polymer matrix promoted by residual nitric acid exists in the EG interlayer. [27]

As shown in **Table 4**, the residue of EG/SPF composites primarily relied on the content of EG. The EG filled SPF exhibited higher residues than the neat foam at high temperature. Moreover, the greater the loading of EG was, the higher the weight of residual will be obtained.

4.6 Dynamic mechanical analysis

As SPF is used as package materials, the damping performance of the SPF composites is of great significance **[28]**. Dynamic mechanical analysis (DMA) is a widely used technique to examine the viscoelastic features of PU foams **[29, 30].** It reveals some key parameters of polymer materials (e.g., the glass transition temperature (T_g), the energy dissipation and the stiffness). Here, the effect of EG particles on the damping properties of the SPFs was measured. The change in loss factor (tan δ) of pure SPF and EG/SPF composites with temperature were presented in **Figure 11.**

Comparing the peak area of the tan δ curve is an effective way of evaluating the damping properties of composite. Larger peak area indicates better damping property. **Table 5** show the peak areas of tanδ curves of EG/SPF composites. It could be found that the addition of the EG leading slight increase on the damping properties. This increase was attributed to not only the increasing energy loss caused by friction between the interfaces of EG and matrix, but also the energy dissipation effect of pore volume when the foams suffer deformation. As the EG content increased, the existed of large numbers of EG particles restricted the deformation of the foam, which

resulting in the decrease of peak area. Meanwhile, due to relatively small cell size, the energy dissipation effect of pores in composite filled with EG-70μm was not significant. The minimum peak area (12.920) was observed for the composite of 50pphp EG-70μm content, as presented in **Table 5.** Moreover, due to the larger surface area and cell size, the EG-960μm/SPF composites had a better damping property compare to the other two systems.

Obtaining the glass transition temperature from the tanδ curves is the most common technique **[31, 32]**. The glass transition temperature (T_g) of the pure foam and the EG/SPF composite, which indicated the peak of tanδ, are listed in **Table 6**. It could be found that addition of the EG reduced the T_g of the composite and the higher the content of EG the lower the value of T_g could be observed.

The decrease in T_g of the composite may be correlated to free volume **[33]**. As we know, EG (especially for the large particle size of EG) have large ratio between surface area and mass. This large specific surface area in the particle/matrix interface created additional free volume which provides more space to the large-scale polymer segments for their easy movements. With the increase of the EG loading from 0 to 50pphp, the free volumes became bigger which results in the further decrease of T_g.

5 CONCLUSIONS

The morphology and properties of semi-rigid polyurethane foam (SPF) filled with three large-span particle sizes (EG-70μm, EG-430μm and EG-960μm) of sulfur-free expandable graphite were investigated.

With the introduction of middle size (EG-430μm) and large size (EG-960μm) EG, the composites presented significant improvement in flame retardant. SPF filled with 50pphp EG-960μm showed the excellent fire behavior with LOI value of 31and vertical burning test of V-0 rating. EG-70μm, however, showed negligible or even negative effect on flame retardant of SPFs.

Thermogravimetric analysis (TGA) showed that EG could significantly improve the thermal stability of SPFs, especially for EG with the larger size and higher content. The loading of EG leaded to a slight increase in damping properties and a decrease in glass transition temperature (T_g) for each sample.

6 ACKNOWLEDGE

7 REFERENCE

1. P. Cinelli, I. Anguillesi, and A. Lazzeri, *Eur. Polym. J.,***49**, 1174 (2013).

2. M.A. Mosiewicki, G.A. Dell'arciprete, M.I. Aranguren, and N.E. Marcovich, *J. Comp. Mat.,***43**, 3057 (2009).

3. D. Q. Chen, J. Y. Yang, and G. H. Chen,*Composites Part A: Applied Science and Manufacturing*, **41**, 1636 (2010).

4. S. Mitsuru, I. Atsushi, and M. Masayoshi,U.S. Patent, 6306,918 Bl (2001).

5. J. Q. Wang, andW. K. Chow, *J. Appl. Polym. Sci.*, **97**, 366 (2005).

6. S.V. Levchik, and E. D. Weil,*Polym. Inter.*, **53**, 1585 (2004).

7. G. Camino, L. Costa, and M. P. Luda,*Makromolekulare Chemie. Macromolecular Symposia,* **74**, 71 (1993).

8. M. S. Dresselhaus, and G. Dresselhaus, *Adv. Phys.,***30**, 139 (1981).

9. J. Li, L. Feng,and Z. Jia, *Mater. Lett.*, **60**, 746 (2006).

10. R. Xie, and B. Qu, *J. Appl. Polym. Sci.*, **80**, 1190 (2001).

11.Z. Z. Li, and B. J. Qu, *Polym. Degrad. Stab.*, **81**, 401 (2003).

12.C. F. Kuan, W. H. Yen, C. H. Chen, S. M. Yuen,H. C. Kuan,and C. L. Chiang,*Polym. Degrad. Stab.,***93**, 1357 (2008).

13. M. Modesti, and A. Lorenzetti, *Polym. Degrad. Stab.*, **78**, 167 (2002).

14.M. Modesti, and A. Lorenzetti, *Eur. Polym. J.,* **39**, 263 (2003).

15. X. G. Zhang,L. L. Ge, W. Q. Zhang, J. H. Tang, L. Ye, andZ. M. Li, *J. Appl. Polym. Sci.*, **122**, 932 (2011).

16. M. Modesti, A. Lorenzetti, F. Simioni, and G. Camino, *Polym. Degrad. Stab.*, **77**, 195 (2002).

17.A. Wolska, M. Goździkiewicz, and J. Ryszkowska, *J. Mater. Sci.*, **47**, 5627 (2012).

18.A. Wolska, M. Goździkiewicz, and J. Ryszkowska,*J. Mater. Sci.*, **47**, 5693 (2012).

19.S. Duquesne, R. Delobel, M. L. Bras, and G. Camino, *Polym. Degrad. Stab.*, **77**, 333 (2002).

20.L. Shi, Z. M. Li, M. B. Yang, B. Yin, Q. M. Zhou, C. R. Tian, and J. Wang, *Polym.*

Plast. Technol. Eng., **44**, 1323 (2005).

21. F. Kang, Y. Leng, and T. Y. Zhang,Carbon, 35, 1089 (1997).

22. M. Thirumal, D. Khastgir, N. K. Singha, B. S. Manjunath, and Y. P. Naik, *J. Appl. Polym. Sci.*, **110**, 2586 (2008).

23. L. Shi,; B. H. Xie, J. H. Wang, C. R. Tian, and M. Y. Yang, *Polym. Int.*, **55**, 862 (2006).

24. X. C. Bian, J. H. Tang, Z. M. Li, Z. Y. Lu, and A. Lu,*J. Appl. Polym. Sci.*, **104**, 3347 (2007).

25. M. Thirumal, D. Khastgir, N. K. Singha, B. S.Manjunath,and Y. P. Naik, *J. Appl. Polym. Sci.*, **108**, 1810 (2008).

26. M. Thirumal, D. Khastgir, N. K. Singha, B. S. Manjunath, and Y. P. Naik,*Cell. Polym.*, **26**, 245 (2007).

27. S. Duquesne, M. L. Bras, S. Bourbigot, R. Delobel, G. Camino, B. Eling, C. Lindsay, and T. Roels, *Polym. Degrad. Stab.*,**74**, 493 (2001).

28. J. Lefebvre, B. Bastin, M. Le Bras, S. Duquesne, R. Paleja, R.Delobel,*Polym. Degrad. Stab.*,**88**, 28(2005).

29. H.Ron, H. Kathy, and A. Randy,*Flexible polyurethane foams*, 2nd ed.,Dow Chemical Co. (1997).

30. B. D. Kaushiva, and G. L. Wilkes,*J. Appl. Polym. Sci.*, **77**, 202 (2000).

31. A. Leszczynska,and K. Pielichowski,*J. Therm. Anal. Calorim.*, **93**, 677 (2008).

32. J. L. Rivera-Armenta, Th. Heinze, and A. M. Mendoza-Martínez,*Eur. Polym. J.*, **40**, 2803 (2004).

33. S. Jana, and W. H. Zhong,*Mat. Sci. Eng.: A*,**525**, 138 (2009).

34. UL-94: Test for Flammability of Plastic Materials for Parts in Devices and Appliances, Underwriters Laboratories Inc. (UL) (2001)

Figure 1 The digital micrographs of EG with different sizes (a, EG-70μm; b,

EG-430μm; c, EG-960μm)

Figure 2 The 'worm-like' structure of the expanded EG

Figure 3 Dynamic rheological analysis results of the component A

Figure 4 Density and compression strength of SPFs with different EG content

Figure 5 SEM micrographs of the pure foam and EG/SPF composites. (a. Pure foam;

b. EG-70μm-50pphp; c. EG-430μm-50pphp; d. EG-960μm-50pphp)

Figure 6 The morphology of EG/SPF composites. (a, EG-70μm-50pphp; b,

EG-430μm-50pphp; c, EG-960μm-50pphp; d, interface between EG flake and foam

matrix)

Figure 7 Limiting oxygen index (LOI) values of the EG/SPF composites

Figure 8 Flame retardant mechanism of EG/SPF composites

Figure 9 Microscope images of the interface of burned 50pphp EG/SPF composites

Figure 10 The TG-DTG curves of the neat and EG filled SPFs

Figure 11 Dynamic mechanical properties of EG/SPF composites

Table 1 Components used in the preparation of EG/SPF composites

Table 2 Effect of EG on mechanical properties of SPFs

Table 3 Results of horizontal and vertical burning tests for EG filled SPFs

Table 4 The TGA data of the EG/SPF composites

Table 5 The peak area of tan δ curve obtained from DMA analysis

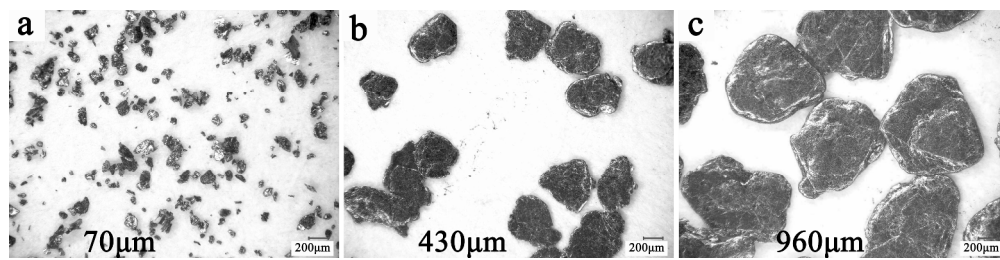**Table 6** The T_g data obtained from DMA analysis

Figure 1 The digital micrographs of EG with different sizes (a, EG-70μm; b, EG-430μm; c, EG-960μm)
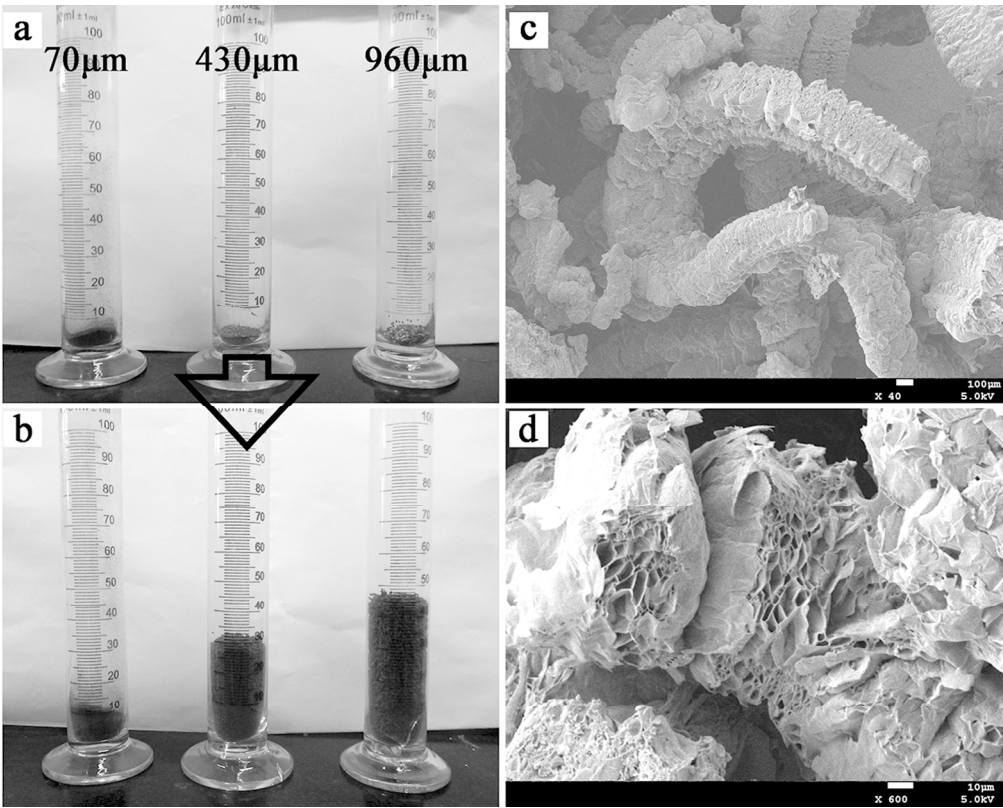410x101mm (300 x 300 DPI)

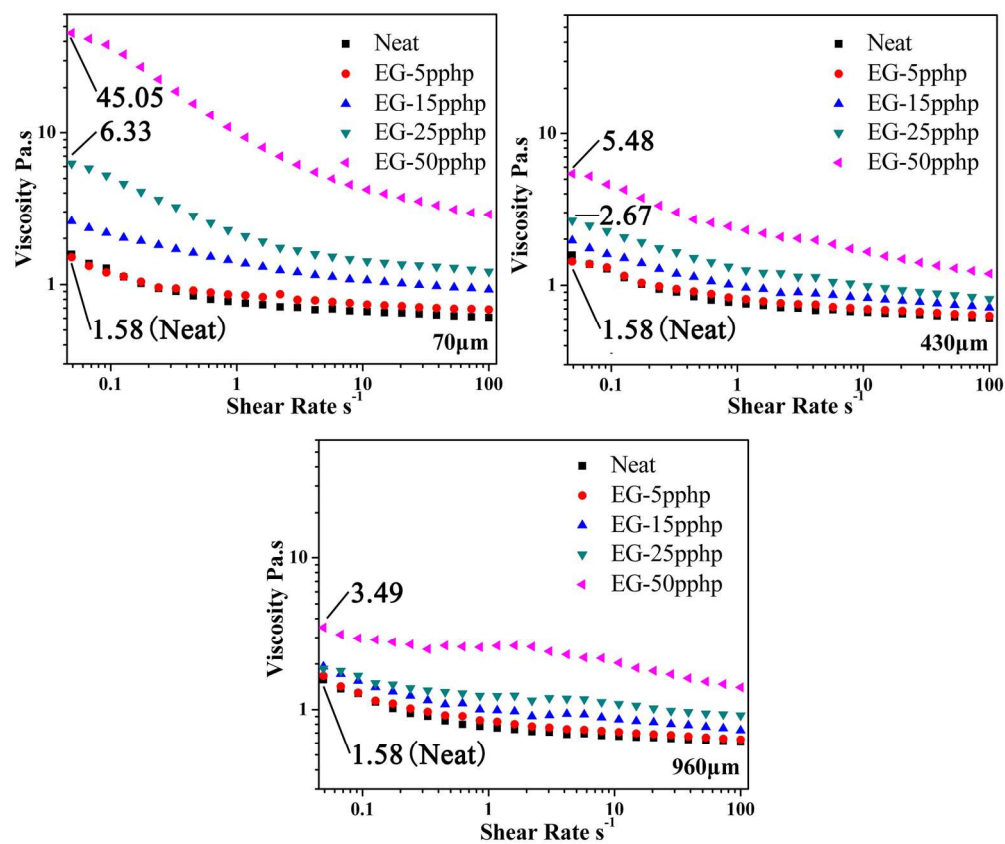Figure 2 The 'worm-like' structure of the expanded EG
109x87mm (300 x 300 DPI)

Figure 3 Dynamic rheological analysis results of the component A
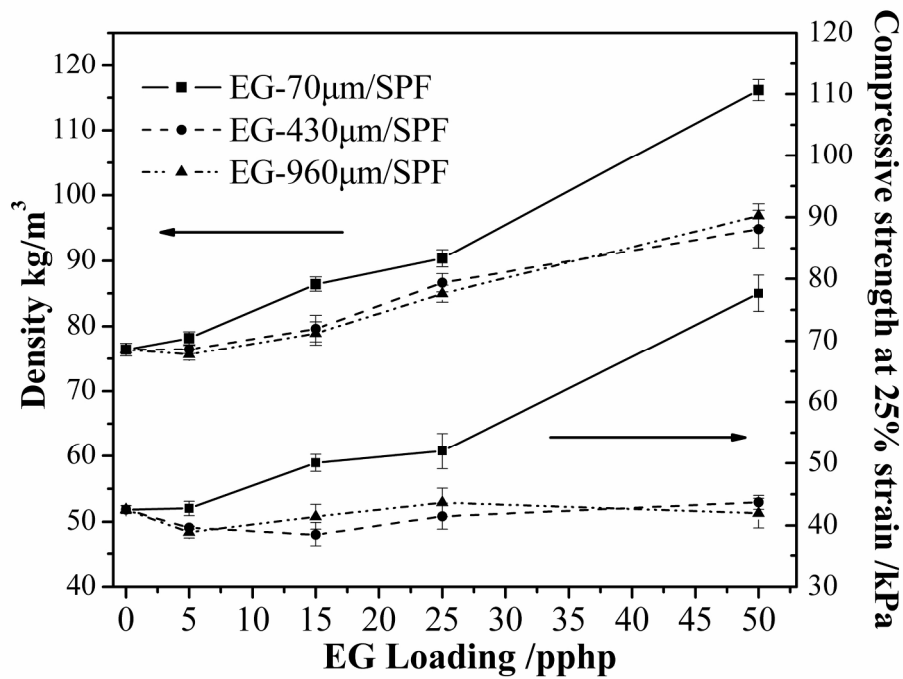171x144mm (300 x 300 DPI)

Figure 4 Density and compression strength of SPFs with different EG content
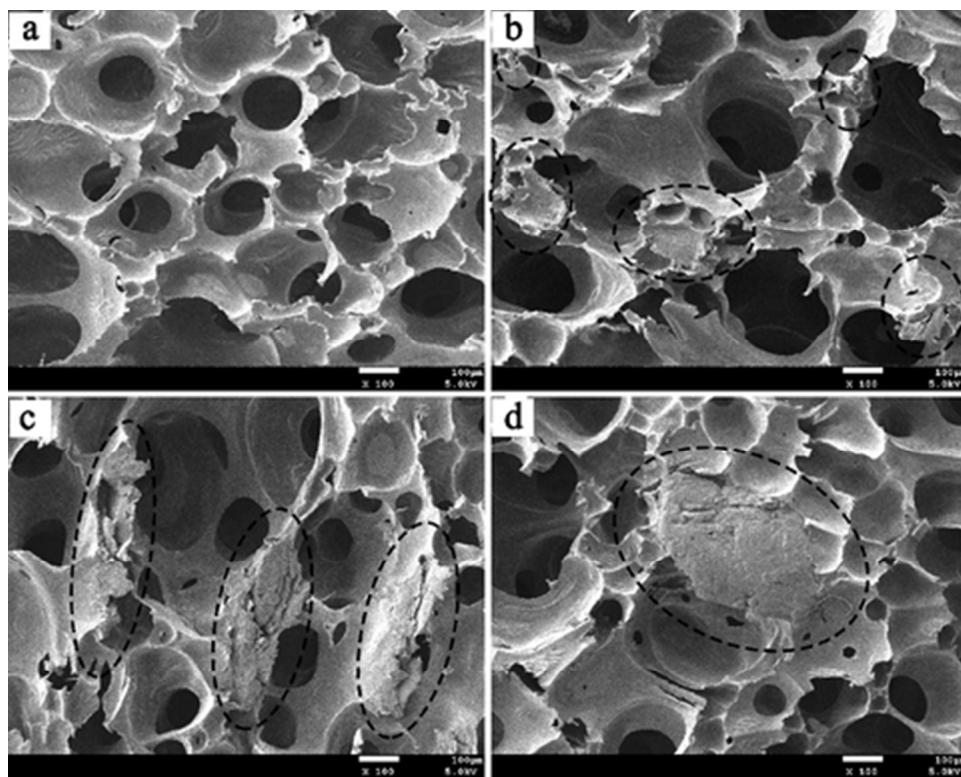215x166mm (300 x 300 DPI)

Figure 5 SEM micrographs of the pure foam and EG/SPF composites. (a. Pure foam; b. EG-70μm-50pphp; c. EG-430μm-50pphp; d. EG-960μm-50pphp)
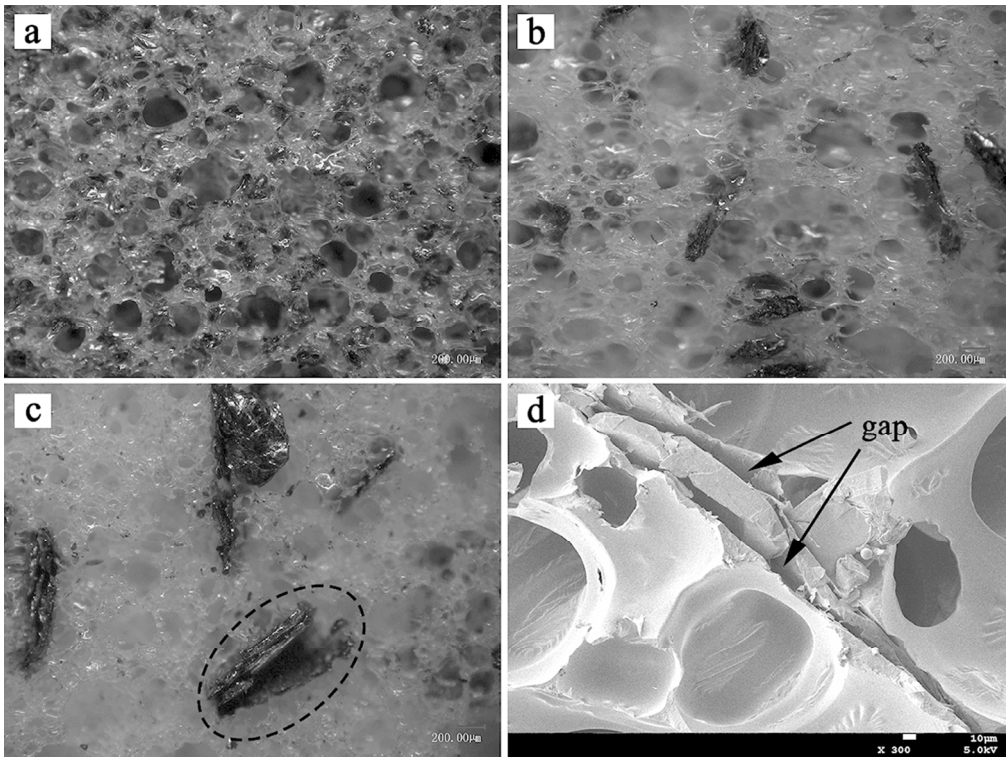40x32mm (300 x 300 DPI)

Figure 6 The morphology of EG/SPF composites. (a, EG-70μm-50pphp; b, EG-430μm-50pphp; c, EG-960μm-50pphp; d, interface between EG flake and foam matrix)
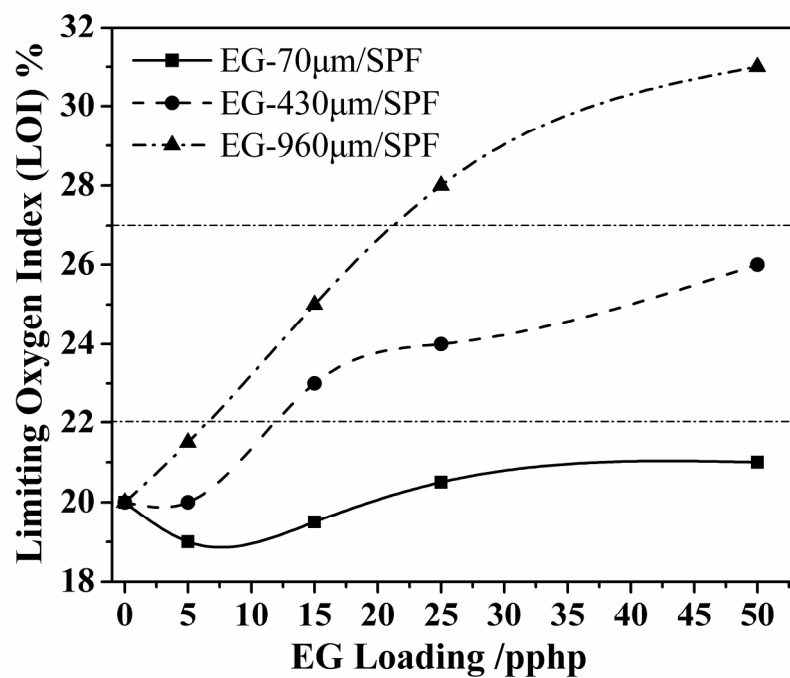101x76mm (300 x 300 DPI)

Figure 7 Limiting oxygen index (LOI) of the EG/SPF composites
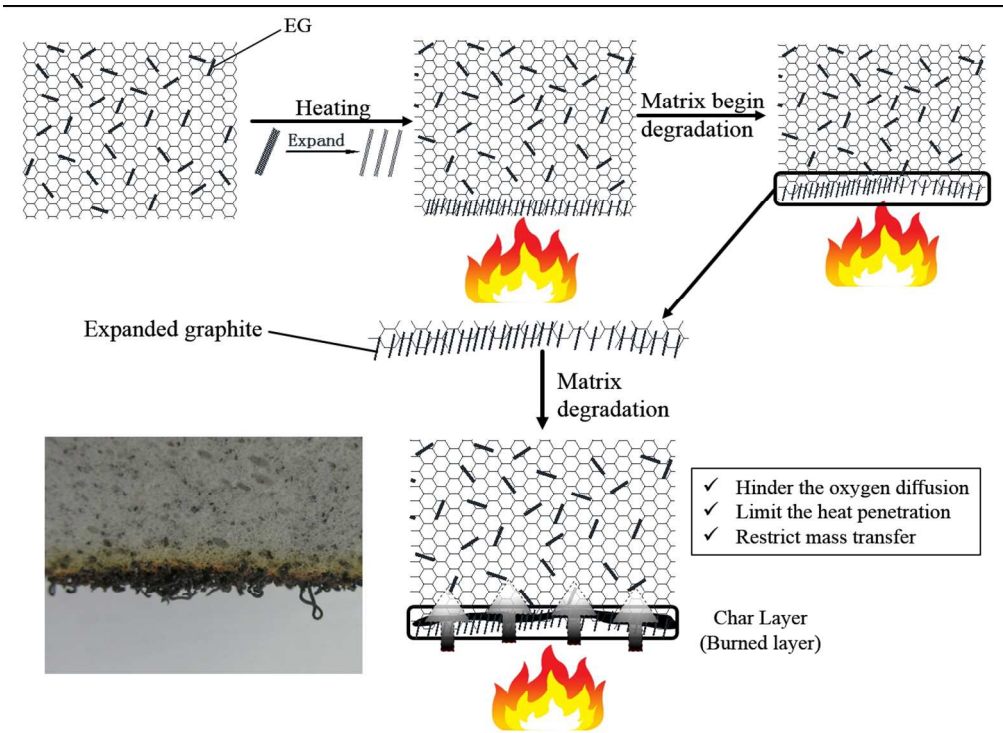215x166mm (300 x 300 DPI)

Figure 8 Flame retardant mechanism of EG/SPF composites
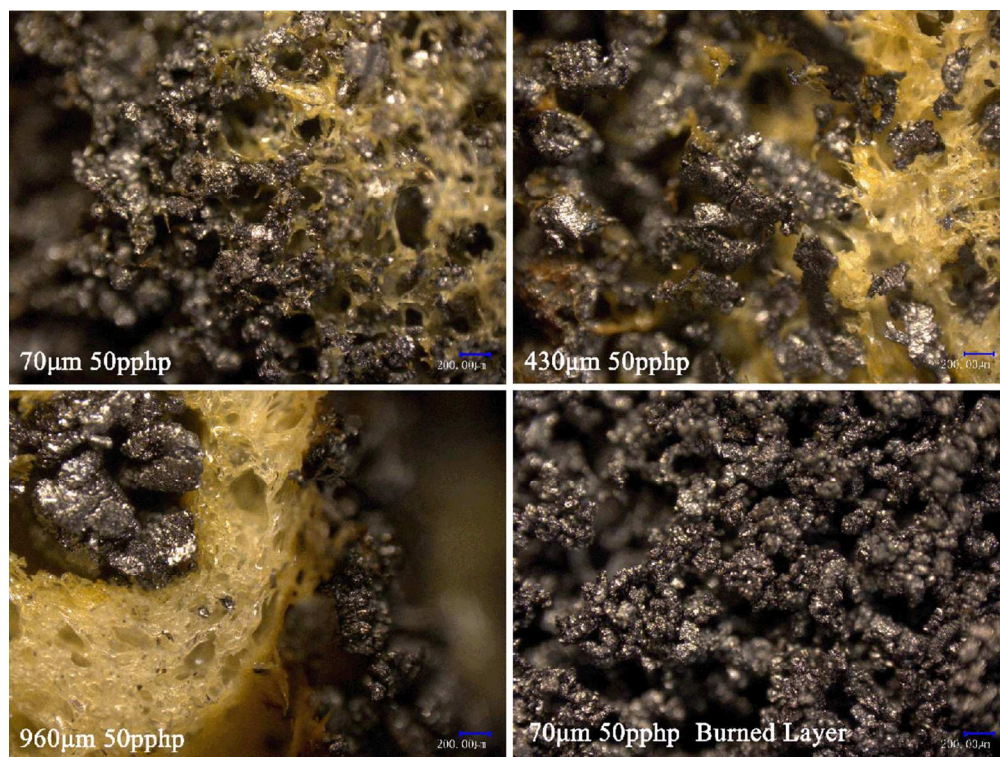238x186mm (150 x 150 DPI)

Figure 9 Microscope images of the interface of burned 50pphp EG/SPF composites
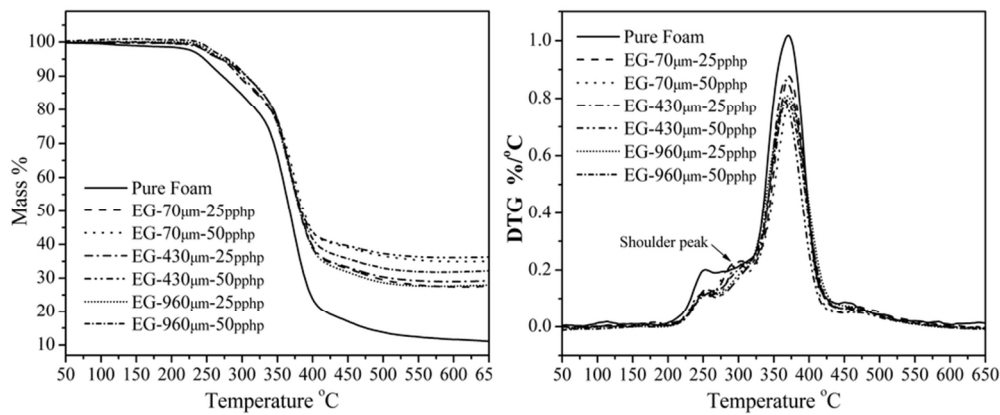101x76mm (300 x 300 DPI)

Figure 10 The TG-DTG curves of the neat and EG filled SPFs
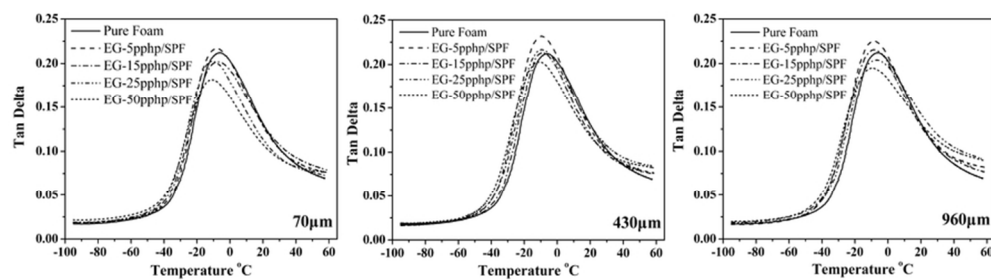83x34mm (300 x 300 DPI)

Figure 11 Dynamic mechanical properties of EG/SPF composites
76x21mm (300 x 300 DPI)

Table 1 Components used in the preparation of EG/SPF composites

Classification	Chemicals	php[*]	% Weight
	Polyol 3050A	100	40.98~51.55
	Chain extender	6	2.46~3.09
	Dabaco DC5188	2	0.82~1.03
Component A	Dabaco 2040	2	0.82~1.03
	Stannous octoate	0.5	0.20~0.25
	Distilled water	2.5	1.02~1.29
	EG (Different particle size)	0~50	20.50~0.00
Component B	PAPI	81	33.20~41.75

[*]*pphp = parts per hundred of polyol by weight.*

Table 2 Effect of EG on the mechanical properties of SPF.

EG content (pphp)	Density (kg/m³)			Compressive strength at 25% strain (kPa)			Specific compressive strength[kPa/(kg/m³)]		
	70μm	430μm	960μm	70μm	430μm	960μm	70μm	430μm	960μm
0		76.42			42.53			0.557	
5	78.19	76.45	75.65	42.72	39.64	38.91	0.546	0.519	0.514
15	86.42	79.63	78.92	50.06	38.52	41.39	0.579	0.484	0.524
25	90.37	86.65	84.96	51.97	41.47	43.69	0.575	0.479	0.514
50	116.18	94.87	96.89	77.67	43.70	41.96	0.669	0.461	0.433

Table 3 Results of horizontal and vertical burning tests for EG filled SPF

Sample	Neat	5pphp	15pphp	25pphp	50pphp
EG-70μm		72.2 mm/min	70.2 mm/min	86.7 mm/min	73.3 mm/min
EG-430μm	72.86 mm/min	56.6 mm/min	[α]HB-3-38.7mm/min	[β]HB-2-9.2mm	[δ]HB-1
EG-960μm		HB-3-39.8mm/min	HB-1	HB-1	HB-1 V-0

[α] *HB-3, the burning rate is less than 40 mm/min.*

[β] *HB-2, the flame front pass the 25 mm reference mark and self-extinguishing.*

[δ] *HB-1, the flame front does not pass the 25 mm reference mark and quenches after the ignition source is removed.*

Table 4 The TGA data of the EG/SPF composites

Sample	Neat	EG-70μm		EG-430μm		EG-960μm	
		25pphp	50pphp	25pphp	50pphp	25pphp	50pphp
$T_{5wt\%}(^{o}C)$	247.0	269.0	271.4	269.8	270.5	275.4	279.6
T_{max} (^{o}C)	369.6	371.9	372.6	366.9	365.7	368.4	367.8
Residue in $650^{o}C$ (%)	11.10	27.6	35.02	29.23	36.23	27.95	32.21

Table 5 The peak area of tan δ curve obtained from DMA analysis

Contents	Peak Area				
	Pure foam	5pphp	15pphp	25pphp	50pphp
EG-70μm/SPF		13.865	13.917	13.430	12.920
EG-430μm/SPF	13.512	14.701	13.538	14.430	14.098
EG-960μm/SPF		14.656	14.444	14.571	14.490

Table 6 The T_g data obtained from DMA analysis

Contents	Glass Transition Temperature (T_g)				
	0	5	15	25	50
EG-70μm/SPF		-7.79	-7.83	-10.78	-11.2
EG-430μm/SPF	-5.9	-9.82	-8.87	-9.65	-11.79
EG-960μm/SPF		-8.88	-8.49	-6.6	-10.12